DESIGN OF HORIZONTAL SHAFT ACTIVE MAGNETIC BEARING SYSTEM

Boštjan Polajžer*, Drago Dolinar*, Gorazd Štumberger*,
Jože Ritonja*, Bojan Grčar*, Kay Hameyer♯

*University of Maribor, Faculty of Electrical Engineering and Computer Science,
Smetanova 17, SI–2000 Maribor, Slovenia, bostjan.polajzer@uni-mb.si

♯KU Leuven, Dept. E.E., Div. ESAT/ELEN, Leuven, Belgium

1 INTRODUCTION

Several principles of magnetic bearings operation are known [1], but the principle based on the use of electromagnets to provide the force necessary for the levitation of a rigid body is the most widely used. The magnetic field has to be adjusted continuously to attain stable levitation and the required dynamics of the levitating body. This can be done only with controlled electromagnets. One application are Active Magnetic Bearings (AMBs) where two pairs of radial bearings controlling four DOFs are placed at each rotor end. The fifth DOF is controlled by a pair of axial bearings. Rotation, i.e. the sixth DOF, is controlled by an independent driving motor. AMBs offer significant advantages due to their non-contact operation. Higher speeds, no friction, no lubrication, weight reduction, precise position control and active vibration damping make them far superior to the conventional bearings. AMBs are therefore a typical mechatronic product and are particularly appropriate for high-speed rotating machines. Commercial applications include pumps, compressors, flywheels, milling and grinding spindles, turbine engines, centrifuges, etc.

The laboratory prototype of an AMB is presented in the paper. The mathematical model of an AMB is determined separately for the mechanical and for the electrical part. The modeling is restricted to the y– axis. The dynamic model with lumped parameters is expressed in the time domain. The model is coupled and nonlinear. The differential driving mode is introduced to avoid the redundancy of input variables. Also, the linearized equilibrium point deviation model is given. Its parameters are determined by the numerical analysis of the magnetic field [2] and by measurements. The obtained model is used for control design [3]. Because of the decentralized control, the same controller parameters are used for the y– axis and for the x– axis. A comparison of experimental and simulation results for the control in y– axis is shown along with experimental results of high speed rotation. Basic mechatronic components of the experimental system are briefly described as well. At the very end, some important findings, difficulties and suggestions with respect to the problem of active vibration damping are summarized.

2 MAGNETIC BEARING SYSTEM MODELING

2.1 Laboratory prototype

In this subsection the mathematical model of the laboratory prototype is presented. The system consists of two axially allocated pairs of electromagnets, i.e. the vertical and the horizontal subsystem. In Fig. 1 a) we can see the schematic presentation of the horizontal–shaft magnetic bearing system with its geometry, and in Fig. 1 b) y– axis of the AMB. The four input variables of the system are voltages on each electromagnet winding. If rotation and elasticity of the shaft are neglected, then the system has two DOFs. The two output variables of the system are shaft positions in the x– and in the y– axis. The determination of the mathematical dynamic model is separated into three steps. First, we write the equations of motion where several geometric relations occur due to the axial allocation of actuators, sensors and weight. The next step of modeling deals with the electromagnets. On the assumption that the iron core and coil windings are idealized we can write the voltage equation for each electromagnet. In the last step we write the equations for the

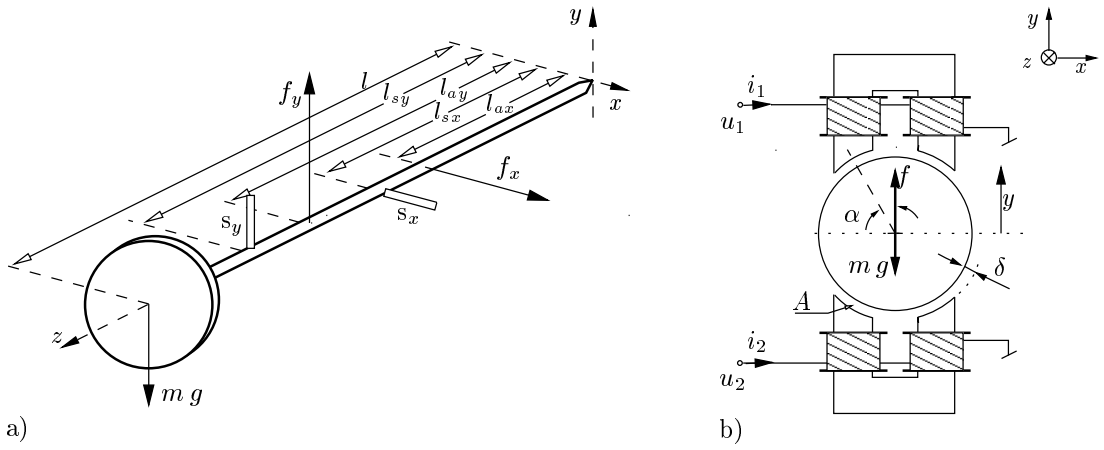

Figure 1: a) *Schematic presentation of the horizontal–shaft magnetic bearing system*, b) y– *axis of the active magnetic bearings*

electromagnetic force generated by each particular electromagnet excited by the coil current. Their sum is the resultant electromagnetic force.

The system has only two independent DOFs, so we will restrict our further discussion to the subsystem describing the y– axis. It consists of two electromagnets with a serially connected pair of coils. The subsystem shown in Fig. 1 b) is described by the mechanical equation of motion (1), two voltage equations (2) where sign of the last term depends on the index (positive sign for $h = 1$, negative sign for $h = 2$) and the equation of the resultant electromagnetic force (3). R is the resistance of one electromagnet, L is the inductance of one electromagnet when the axis of the shaft is in the center. k [Nm^2/A^2] is the force coefficient and k_u [Vs/m] the coefficient of the back–EMF. The nominal air gap and equivalent shaft mass are denoted with δ and m respectively.

$$m\frac{d^2y}{dt^2} = f - m\,g \pm f_l \tag{1}$$

$$u_h = i_h R + L\frac{di_h}{dt} \pm k_u\frac{dy}{dt} \quad ; \quad h = 1, 2 \tag{2}$$

$$f = k\left(\frac{i_1^2}{(\delta - y)^2} - \frac{i_2^2}{(\delta + y)^2}\right) \tag{3}$$

The AMB model given in the form of equations (1), (2) and (3) is multi-variable, coupled and nonlinear. Let us assume constant model parameters. Voltages u_1 and u_2 are system inputs, the position y is the output, and the common disturbance consists of the equivalent gravity force mg and the load force f_l. If we bear in mind that the system is totally controllable the redundancy of input variables becomes evident. For its elimination we introduce the differential driving mode. The bias current i_0 is forced through the coils of both electromagnets. Considering the given assumptions the resultant electromagnetic force f_0 is zero. But as we know there always exist the load force f_l and the disturbances as well as the gravity force mg, we have to add the so-called control current ($i_\Delta \leq i_0$) in the upper coil and subtract it in the lower coil (4). In this way a SISO system is obtained where the input variable is the so-called control voltage u_Δ or the control current i_Δ in case of a current fed system.

$$i_1 := i_0 + i_\Delta, \qquad i_2 := i_0 - i_\Delta \tag{4}$$

2.2 Linearized equilibrium point deviation model

Among the model equations (1), (2) and (3), only equation (3) is nonlinear. It is linearized in the equilibrium point (i_0, y_0) where i_0 is an arbitrary bias current and y_0 the position of the shaft's axis

in the center ($y = 0$). Taking into account the first term of the Taylor expansion of equation (3) about the equilibrium point the electromagnetic force is given by the well-known linear equation (5). The current gain coefficient k_i [N/A] and the position stiffness coefficient k_y [N/m] are defined as (6). After rearranging equations (1), (2) and (5) the linearized AMB model is obtained (7). The equivalent model in the input-output domain is defined by the transfer function (8).

$$f_\Delta = k_i\, i_\Delta + k_y\, y_\Delta \tag{5}$$

$$k_i := \left.\frac{\partial f}{\partial\, i_\Delta}\right|_{(i_0,y_0)} = 4k\,\frac{i_0}{\delta^2}, \qquad k_y := \left.\frac{\partial f}{\partial\, y_\Delta}\right|_{(i_0,y_0)} = 4k\,\frac{i_0^2}{\delta^3} \tag{6}$$

$$\begin{aligned} k_i\, i_\Delta + k_y\, y_\Delta - m\frac{d^2 y_\Delta}{dt^2} &= 0 \\ Ri_\Delta + L\frac{di_\Delta}{dt} + k_i\frac{dy_\Delta}{dt} - u_\Delta &= 0 \end{aligned} \tag{7}$$

$$G(s) = \frac{Y_\Delta(s)}{U_\Delta(s)} = \frac{k_i}{mL\,s^3 + mR\,s^2 + (k_i^2 - k_y L)\,s - k_y R} \tag{8}$$

$$G_{mech}(s) = \frac{Y_\Delta(s)}{I_\Delta(s)} = \frac{k_i}{m\,s^2 - k_y} \qquad G_{el}(s) = \frac{I_\Delta(s)}{U_\Delta(s)} = \frac{m\,s^2 - k_y}{mL\,s^3 + mR\,s^2 + (k_i^2 - k_y L)\,s - k_y R} \tag{9}$$

The parameters of the linearized equilibrium point deviation model of the laboratory prototype of active magnetic bearings are shown in Table 1. Current gain and position stiffness are calculated by the numerical analysis of the magnetic field [2] using the finite element method (FEM). The calculated results have been compared with the measured values.

Table 1: *Parameters of the linearized model in equilibrium point* (i_0, y_0)

data	parameter	value	determination
resistance	R [Ω]	0.6	measured
inductance	L [H]	0.0048	measured
equivalent mass	m [kg]	5	measured
current gain	k_i [N/A]	32.7	FEM
position stiffness	k_y [N/m]	108350	FEM
bias current	i_0 [A]	2.5	free parameter
nominal air gap	δ [m]	$0.6 \cdot 10^{-3}$	construction data

3 CONTROL

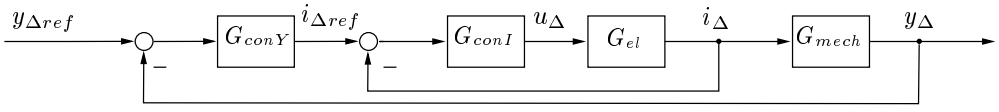

Figure 2: *Control structure of the system*

This AMB represents unstable system, therefore we need a closed-loop control system to stabilize it. The cascade structure has been used (Fig. 2). In the inner loop the current controller $G_{conI}(s)$ is responsible for the best possible reference current tracking. Let us assume that the latter is perfect. Then it is enough to use only the mechanical transfer function $G_{mech}(s)$ (9), defined by two real poles ($s_{1,2} = \pm 164.58$), for the further position controller design. A PID controller (10) has been used for stabilization purposes. Its parameters are defined by increasing the amplitude of the

frequency characteristic at low frequencies, and by trying to attain an adequate phase margin for the chosen cross frequency in case of high frequencies. As the system consists of two independent DOFs decentralized control has been implemented. Therefore the same controller parameters has been used also for the x– axis. The position controller was set up as follows: controller gain $K_{con} = 10000$, integral time constant $T_i = 0.03$ s, derivative time constant $T_d = 0.003$ s and parasitic derivative time constant $T_d' = T_d/10$.

$$G_{conY}(s) = K_{con} \frac{s\,T_i + 1}{s\,T_i} \frac{s\,T_d + 1}{s\,T_d' + 1} \tag{10}$$

4 SIMULATION AND EXPERIMENT

In simulations (MATLAB – Simulink) all parts of the experimental system shown in Fig. 3 a) were considered in addition to the nonlinear actuator model (Fig. 3 b). Let us describe some parts of the system. First, the inductive position sensor with a sensitivity of 7.7 mV/μm and 20 kHz cut-off frequency was chosen very carefully. An additional filter for sensor cross-talk elimination was implemented afterwards at 5 kHz. Next, the analogue current controller and a 20 kHZ PWM switching amplifier were used with a 300 VA per channel. Finally, the digital PID position controller with anti-windup was implemented into the power PC environment with a sampling time of 100 μs.

a) b)

Figure 3: a) *Experimental system and* b) *laboratory prototype AMB*

Fig. 4 shows the comparison of calculations and measurements on the laboratory prototype. Only the comparison of control in the y– axis is shown. It is obvious that the agreement of results is very good – excellent damping agreement and acceptable stiffness disagreement. However, the result for the stability test was quite different. The upper stability limit of the experimental system was much lower than the one we established theoretically. This means that we can not achieve a very high stiffness. The reason for this are the actuator limitations. As a result, insufficient forces are generated for a wide range of shaft positions. This conclusion is confirmed by FEM calculations and measurements of the $f(i_\Delta, y)$ relation. In Fig. 5 the results of the rotation test, where the position error does not exceed ± 15 μm, are also presented. In Fig. 5 b) the shaft elasticity problem turns up in addition to the rotor unbalance problem which is more evident in Fig. 5 c).

5 CONCLUSION

The paper deals with the modeling and the analysis of AMB laboratory prototype. If we take into account that the system has two independent DOFs, then the analysis of the model is restricted to the y– axis. The differential driving mode is introduced and the linearized equilibrium point deviation model is written. Its parameters are measured and calculated by the numerical analysis of the magnetic field. The PID controller design of the y– axis is included. Because of the decentralized control, the same control design is used also for the x– axis.

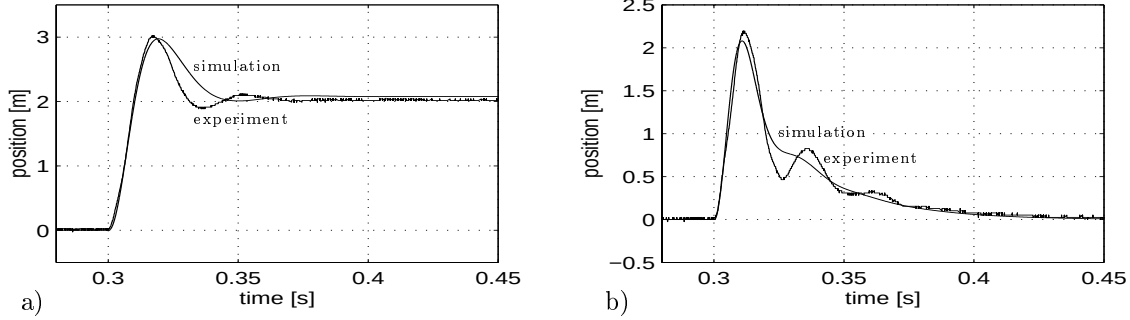

Figure 4: *The position response of y– axis from the equilibrium point:* a) *to the reference step function* (0.2 mm) *and* b) *to the load step function* (60 N)

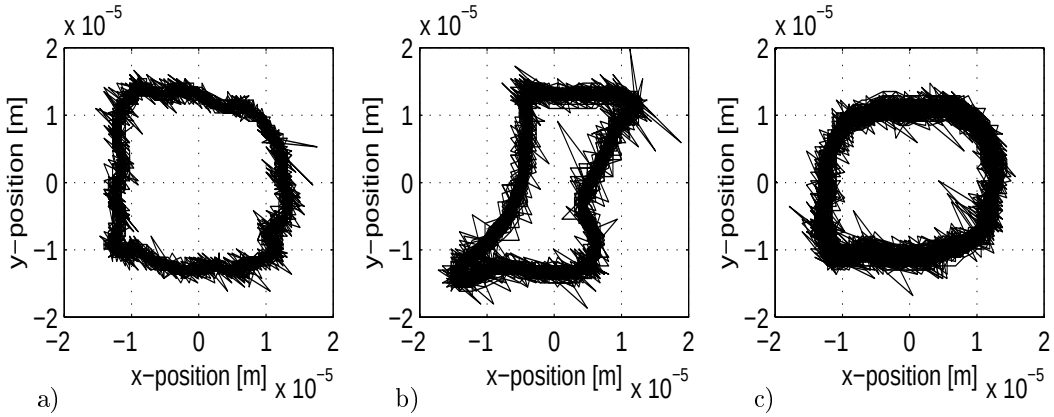

Figure 5: *The experimental position response:* a) *at* 3890 rpm, b) *at* 6600 rpm *and* c) *at* 8040 rmp

The presented work represents one of the first steps in the research of modeling, analysis and control design of AMB at our institution. Although we used one of the most simple control methods we came to the following important conclusions:

- the rigidity of the system is increased by a higher bias current i_0 and controller gain K_{con}
- the system dynamics is improved by an appropriate derivative time constant T_d
- the influence of disturbances is reduced by an appropriate integral time constant T_i
- the system stiffness insufficiency is caused by actuator limitations, therefore an appropriate actuator should be carefully chosen with respect to the expected load forces and available power supply or vice versa
- the non-modeled dynamics of the shaft elasticity and unbalanced rotor becomes evident at the so-called critical speeds and this is why the control design for active vibration damping should also employ the non-modeled rotor-dynamics.

Acknowledgments

The authors are grateful to the Belgian Federal office for scientific, technical and cultural affairs for promoting the W&T cooperation with Central- and East Europe by giving the DWTC grant to D. Dolinar. Thanks are due to the Ministry of Science and Technology of Slovenia for the financial support.

References

[1] G. Schweitzer, H. Bleuer, and A. Traxler, *Active Magnetic Bearings – Basics, Properties and Applications of Active Magnetic Bearings.* Zürich: VDF, 1994.

[2] *Olympos - Finite Element and Optimization Package*, see http://www.esat.kuleuven.ac.be/elen/elen.html, online help.

[3] C. Knospe, "PID control for magnetic bearings," in *Short Course on Magnetic Bearings, Lecture 7*, (Alexandria, Virginia), 1997.